Talanta 82 (2010) 528–533

Contents lists available at ScienceDirect

Talanta

journal homepage: www.elsevier.com/locate/talanta

Magnetic bead based immunoassay for enumeration of CD4+ T lymphocytes on a microfluidic device

Dan Gao[a,b], Hai-Fang Li[b], Guang-Sheng Guo[a], Jin-Ming Lin[b,*]

[a] State Key Laboratory of Chemical Resource Engineering, Beijing University of Chemical Technology, Beijing 100029, China
[b] Department of Chemistry, Tsinghua University, Beijing 100084, China

ARTICLE INFO

Article history:
Received 4 February 2010
Received in revised form 6 May 2010
Accepted 8 May 2010
Available online 19 May 2010

Keywords:
Microfluidic device
Magnetic beads
Cell separation
CD4+ T lymphocytes enumeration

ABSTRACT

Human immunodeficiency virus (HIV) diagnostics are urgently needed in resource-scarce settings. Monitoring of HIV-infected patients requires accurate counting of CD4+ T lymphocytes. However, the current methods for enumeration of CD4+ T lymphocytes are of high cost, technically complex and time-consuming. In this paper, we developed a simple, rapid and inexpensive one-step immunomagnetic method for separating and counting CD4+ T lymphocytes on microfluidic devices with enlarged reaction chambers. CD4+ T lymphocytes were successfully separated and captured from the cell suspension obtained from mouse thymus. CD4 counts were determined under an optical microscope in a rapid and simple format. In order to acquire the maximum efficiency of cell capture, relative parameters were investigated, including section area of the reaction chamber and injection flow rate of the cell suspension. The enlarged reaction chamber with two symmetrical cone-shaped ends was helpful for cell capture, and the maximum capability of captured CD4+ T lymphocytes was about 700 cells μL^{-1}. Our investigations avoided the complex sample pre-treatment, and the entire analysis time was significantly reduced to 15 min. This CD4 counting microdevice had the potential to reduce the cost for HIV diagnosis in resource-limited settings.

1. Introduction

It has been widely recognized that the amount of people infected with human immunodeficiency virus (HIV) has been increasing in recent years, especially in developing countries. Thus, there is an urgent need for rapid diagnosis, monitoring and antiretroviral therapy. The absolute number of CD4+ T lymphocytes per microliter of blood is one of the most important biological markers for determining disease progression and monitoring efficacy of the treatment [1]. Clinically, a CD4+ T lymphocyte count of less than 200 cells μL^{-1} is recommended as a criterion for AIDS. Besides, the ratio of CD4+ T lymphocytes to the total lymphocytes is also an important parameter, especially in paediatric HIV infection [2]. In developed countries, the counts of CD4+ T lymphocytes are usually performed every 3–6 months for HIV-infected patients with flow cytometry, which is currently considered as the standard reference method for enumeration of absolute CD4+ T lymphocytes [3]. The reliable method can be used for high throughput assays, but the technical and operational complexity, highly trained personnel and high cost of reagents make it difficult and impractical to sustain in many developing countries.

Several efforts have been made to develop low-cost and simple methods to count T lymphocyte subsets. For example, some non-cytofluorometric methods including Enzyme-Linked Immunosorbent Assay (ELISA) [4–6] and immunomagnetic separation methods [7,8] have been recommended as useful alternatives for CD4+ T lymphocyte enumeration. But these methods still showed disadvantages, such as high cost, low accuracy and low throughput. In this context, microfluidic device provided an excellent platform for cellular and subcellular analysis with lower cost and complexity [9–12]. In recent years, several methods, such as magnetic separation format [13–15] and electrical method [16–20] have been used on-chip for the enumeration of T lymphocyte subsets in laboratories with limited facilities.

Many studies have demonstrated that miniaturized equipments could be integrated to microfluidic devices to conquer the drawbacks of conventional flow cytometers. Wang and co-workers [21] established an integrated microfluidic device for flow cytometry and fluorescence activated cell sorting based on gravity and electric force driving of cells. Sturm and co-workers [22] developed a simple method to measure the hydrodynamic size of cells using an array of posts integrated on a microfluidic device. The sizes of cells were determined by the degree of lateral displacement which was different from forward scatter in conventional flow cytometry. Furthermore, a few examples on miniaturized CD4 counting systems have been reported. A bioactivated polydimethylsiloxane (PDMS)

* Corresponding author. Tel.: +86 10 62792343; fax: +86 10 62792343.
E-mail address: jmlin@mail.tsinghua.edu.cn (J.-M. Lin).

0039-9140/$ – see front matter © 2010 Elsevier B.V. All rights reserved.
doi:10.1016/j.talanta.2010.05.019

microchannel with biosensor surface was explored by Bergquist and co-workers to separate and count CD4+ T lymphocytes, a simple fluorescence microscope was the only equipment needed for detection [23]. Rodriguez et al. reported a low-cost and simple method by integrating a separation membrane on a flow cell to separate the stained CD4+ T lymphocytes from the red blood cells [24]. Toner and co-workers developed a functional microfluidic device by coating the microchannels with anti-CD4 antibodies to capture the unlabeled CD4+ T lymphocytes with high efficiency [25,26]. However, antibody-coated walls did not give highly reproducible efficiency for cell capture. Magnetic activated cell sorting could overcome the defects of previous cell sorting methods because the antibody-coated magnetic beads offered a large specific surface area for chemical binding and they could be magnetically manipulated using external permanent magnets or electromagnets. Magnetic beads have been successfully applied on microfluidic devices for cell isolation with higher capture efficiency than antibody-coated microchannels [13,27,28].

In this paper, we presented a simple microfluidic device with an enlarged reaction chamber for CD4+ T lymphocytes capture. Compared with the CD4 separation methods in the literatures (such as antibody-coated microfluidic device or magnetic activated cell sorting), our device had a simpler chip design and higher cell capture efficiency. In addition, the formation of magnetically trapped bead bed for cell capture had several other advantages, such as short analysis time, minimal sample consumption, higher reproducibility and reusability of the microfluidic device. Due to the interaction time of antibody-coated magnetic beads with antigen of cells strongly influenced the cell capture efficiency, crucial parameters such as section area of the reaction chamber and injection flow rate of cell suspension were investigated to obtain the maximum cell capture efficiency. Compared to the similar experiments performed off-line, we demonstrated a more convenient method to separate and count CD4+ T lymphocytes on microfluidic device that can be used in resource-limited settings.

2. Experimental

2.1. Chemicals and reagents

All chemicals were analytical grade and were used without further purification. For the lymphocyte suspension preparation, several healthy female ICR mice aged 4–5 weeks, weighing 200–220 g were purchased from Beijing Weitong Lihua Experimental Animal Technical Corp. (Beijing, China). A 300-mesh cell screen was obtained from Shiji Yinfeng Technology Development Corp. (Beijing, China). Anti-mouse CD4 paramagnetic beads were purchased from Invitrogen Corp. (Carlsbad, USA). Bovine serum albumin (BSA) and hydroxypropyl methylcellulose (HPMC) were obtained from Sigma–Aldrich (Buchs, Switzerland). Trypan blue was purchased from Xin Jing Ke Biotechnology Corp. (Beijing, China). For microchip fabrication, SU-8 photoresist (SU-8 2050) and developer (propylene glycol methyl ether acetate, PGMEA) were obtained from MicroChem (Newton, MA, USA). PDMS and curing agent were purchased from Dow Corning (Midland, MI). 3 in. silicon wafers were purchased from SCHOTT Guinchard (Yverdon, Switzerland). NdFeB permanent magnet plates with 6 mm diameter (290 mT) were obtained from Yingke Hongye Technical Corp. (Beijing, China).

2.2. Microchip design and fabrication

The Y-intersection microfluidic devices with five different sizes of reaction chambers were designed in this work. The design and dimensions of the devices are shown in Fig. 1. The different widths of the reaction chambers changed from 200 μm to 1 mm in interval of 200 μm, and the length of the five reaction chambers was 2 mm. The reaction chamber with two symmetrical cone-shaped ends aimed to reduce dead-volumes or liquid retention in the corners [29]. The microfluidic device with two inlets was used to introduce cell suspension and magnetic beads separately. Meanwhile, it can avoid sample cross-contamination. The microchannels were fabricated according to standard soft photolithography and replica molding techniques [30]. Briefly, SU-8 2050 negative photoresist was spin-coated on a 3 in. silicon wafer at 2200 rpm for 1 min to achieve a homogenous layer of 65 ± 2 μm. The patterns were exposed with UV-light through a high-definition transparent mask and then baked at 60 °C, unexposed photoresist was rinsed with PGMEA. The wafer was silanized for 1 h with Trichloro(1H,1H,2H,2H-perfluoroctyl) silane evaporated in a desiccator to decrease the adhesion of PDMS to the master during molding. A 10:1 weight mixture of PDMS prepolymer and curing agent was degassed in vacuum to remove air bubbles generated during mixing. The mixture was then poured on the master and baked in an oven at 80 °C for 2 h. The cured PDMS replica was peeled off from the wafer and the connection holes were punched with a syringe tip. The PDMS replicas were irreversibly sealed with cover glasses sheet by oxygen plasma for 90 s. The channels were rinsed with ethanol and sterile deionized water to remove debris or dust before use.

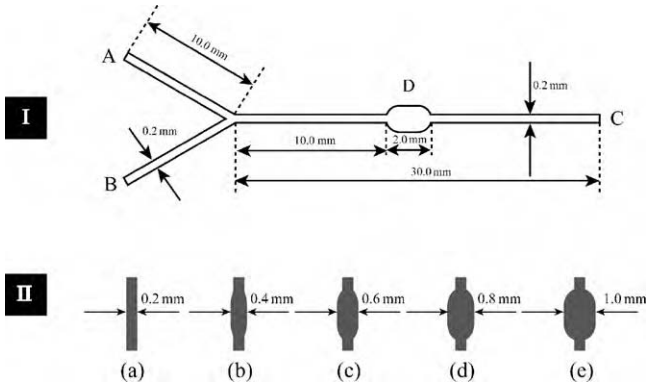

Fig. 1. Schematics of the Y-intersection microchip (I) with different sizes of reaction chambers (II) used in this study. Dimensions (in mm) correspond to the photomask features. A and B represent the inlets; C represents the outlet; D represents the reaction chamber. Five microchannels with the same depth but different widths were fabricated on the microchip.

2.3. Sample preparation

Lymphocyte suspension was acquired from thymus of ICR mouse. Thymus tissues were isolated from mouse under sterile conditions. The tissues were rinsed three times in PBS, placed in PBS in a sterile glass Petri dish and cut softly into small pieces. After that, the cell suspension was filtered by 300-mesh cell screen, then centrifuged at 1000 rpm for 5 min and resuspended in PBS (pH 7.4) to remove dead cells and cell debris. Cells were counted with a hemocytometer, and the cell concentration was kept between 1.0×10^5 cells mL^{-1} and 1.0×10^7 cells mL^{-1}. The cell viability was determined using 0.4% trypan blue solution. Serial dilutions were performed with PBS containing 0.4% HPMC. The cells were analyzed within 24 h after collection.

2.4. Off-chip cell isolation

The CD4+ T lymphocytes were isolated from lymphocyte suspension using magnetic beads coated with anti-mouse CD4 antibody. Briefly, 75 μL of the magnetic beads was added to 100 μL

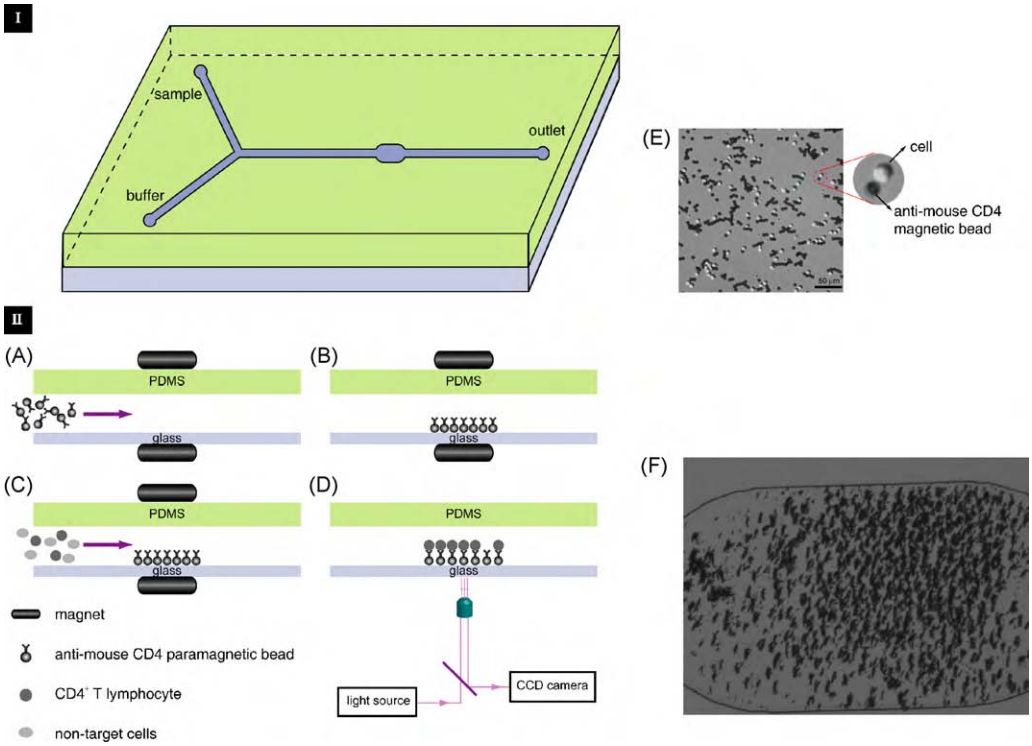

Fig. 2. Schematic view of a bonded Y-intersection microchip (I) and schematic diagram of an immunomagnetic separation of $CD4^+$ T lymphocytes in the reaction chamber (II). (A and B) Anti-mouse CD4 magnetic beads were pumped into the channel and captured with two magnets. (C) Lymphocyte suspension was introduced from two inlets, and then flushed the microchannel with PBS. (D) Magnets were removed and captured cells were imaged under an inverted microscope equipped with a CCD camera. (E) An image of $CD4^+$ T lymphocytes captured by magnetic beads in the reaction chamber. (F) Anti-mouse CD4 paramagnetic beads were captured in the reaction chamber under an asymmetric magnetic field.

of lymphocyte suspension, the mixture was then incubated for 20–30 min at room temperature on a Dynal mechanical rotator, the beads were separated by a magnetic particle concentrator and washed twice with PBS. The captured cells were then counted manually under an inverted microscope. Additionally, the supernatant solution was collected and mixed with magnetic beads, then repeated with the above procedures. In order to determine the cell capture efficiency, we compared the captured cells in the supernatant and lymphocyte stock suspension, and the cell capture efficiency was calculated by the ratio of captured cells in the stock suspension to captured cells in the supernatant and in the stock suspension. The cell capture efficiency was found to be $93.7 \pm 2.2\%$. The total analysis time for off-chip isolation was about 1 h. It was demonstrated that this antibody-coated magnetic bead separation method was reliable in isolation of $CD4^+$ T lymphocytes.

2.5. On-chip operating procedures

After devices were rinsed with ethanol and water, channels were flushed with PBS containing 1% BSA at a flow rate of 5 μL min^{-1} for 10 min to block non-specific adsorption. Anti-mouse CD4 paramagnetic beads were firstly washed 3 times by PBS containing 0.1% BSA (w/v) before use. 2 μL of the beads suspension was then introduced into microchannels at a controlled flow rate using a syringe pump (Harvard Apparatus PHD 2000, Holliston, MA) and magnetically immobilized in the chamber with two permanent magnets below and above the reaction chamber (Fig. 2A and B). Hamilton gastight syringe connected with Teflon tube was pre-filled with PBS, then 1 μL of lymphocyte suspension was drawn into its end of tube. The lymphocyte suspension was pumped into the channel for 15 min at a certain flow rate (Fig. 2C). Subsequently, the chamber was flushed with PBS containing 0.1% BSA at 6 μL min^{-1} for 5 min to wash away the unbound cells. $CD4^+$ T lymphocytes were captured with the magnetic beads due to the interaction of antibody and cell surface antigen. After removing two magnets, captured $CD4^+$ T lymphocytes were imaged under an inverted microscope equipped with a CCD and manually counted. This step should be operated carefully to avoid the bead bed destruction (Fig. 2D). An image of $CD4^+$ T lymphocytes captured with magnetic beads was shown in Fig. 2E. Magnetic beads were about 4.5 μm in diameter, cells were about 10 μm. The magnetic beads were dispersed well in the reaction chamber (Fig. 2F). It was realized by manually moving the magnets back and forth along the direction of the channel. This step was also applied in the following experiments.

3. Results and discussion

3.1. Magnetic beads capture

Initial formation of the bead bed was an important step in preparing the device for sample capture and enrichment, and we designed five reaction chambers with different dimensions to investigate the magnetic bead capture efficiency. Before magnetic beads introduction, the microchannels should be washed carefully to avoid bubble formation. The flow rate for the capture of magnetic beads could be increased by placing two symmetrical magnets on both sides of the reaction chamber. The maximum flow rate for the capture of magnetic beads (100%) was measured using the five microfluidic devices. The results shown in Fig. 3 indicate a good linear relationship between section area (A) of reaction chamber and flow rate (u). The fitting formula was $A = 2.62 + 2.16 \times 10^{-1} u$ with an r^2 of 0.996.

The experiments were performed using 2 μL of antibody-coated magnetic beads. Each data point was repeated at least 3 times in a same device. In order to determine the shear force acting on the cells, we measured the viscosity (6.28×10^{-3} Pa s at 20 °C) of the cell

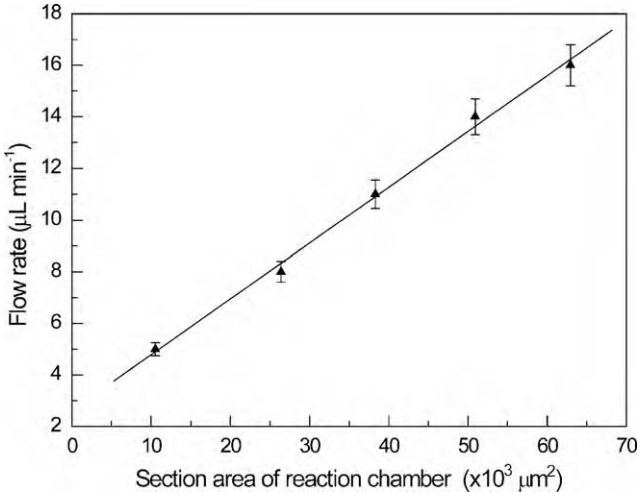

Fig. 3. Effect of section areas on the maximum liquid flow rate to capture all the beads in five different sizes of micro-devices. There is a linear correlation between them ($r^2 = 0.996$, $Q = 2.62 + 2.16 \times 10^{-1} V$). The experiments were performed using 2 μL of antibody-coated magnetic beads. The standard error bars mean the variation of three individual experiments in a same device.

suspension according to the method of capillary electrophoresis [31]. The shear stress, τ(cell), was calculated by the Eq. (1) [32]

$$\tau(\text{cell}) = \frac{6Q\mu}{h^2 w} \quad (1)$$

where Q is volume flow, μ is fluid viscosity, h and w are the height and width of the microchannel. The maximum flow rate measured in the largest reaction chamber was about 16 μL min^{-1} (corresponding shear stress, 64 dyn cm^{-2}), while in the smallest reaction chamber was about 5 μL min^{-1} (corresponding shear stress, 20 dyn cm^{-2}). According to the basic Eq. (2) for the principle of fluid movements, when the fluid flowed from the main channel to the reaction chamber, the section area of the reaction chamber (A) becomes larger, and the flow rate (u) becomes lower. If the reaction chamber was further increased, the flow rate in the reaction chamber could be even lower.

$$Q = Au \quad (2)$$

It is indicated that the hydrodynamic forces applied on the magnetic beads could be reduced in the largest reaction chamber so that the beads could be easily captured. Meanwhile, it had a wider range of flow rate to capture the beads and to wash the unbounded cells in the larger micro-device. Due to the same magnetic field force applied on the magnetic beads, the maximum flow rate for the capture of magnetic beads was the same. As a result, Q is proportional to A. In the following experiments, 2 μL of antibody-coated magnetic beads (1×10^8 beads mL^{-1}) was delivered into the microchannel at a flow rate of 10 μL min^{-1}. The bead introduction required less than 1 min and they could be thoroughly dispersed in the reaction chamber by manually moving the magnets back and forth along the direction of the channel. The thoroughly dispersed beads were helpful for sufficient contact of cell suspension with antibody-coated magnetic beads to improve the cell capture efficiency.

3.2. Effect of reaction chamber dimensions on CD4⁺ T lymphocyte capture efficiency

As the velocity only decreased in the reaction chambers, the interaction time of antibody-coated magnetic beads with antigen of cells could be increased. We further investigated the dynamic cell adhesion behaviour in different reaction chambers. The flow rate for cell injection was kept at 0.1 μL min^{-1}, but the flow rate in the five reaction chambers was different caused by different section areas of the chambers. Using 1 μL cell suspension with the concentration of 7.4×10^6 cells mL^{-1} as a sample, the absolute number of captured CD4⁺ T lymphocytes was investigated in different microfluidic devices.

Several characteristics of cells in aqueous solution, such as adsorption to uncoated glass channels and sedimentation, are troublesome for on-chip manipulation and analysis. Kovac and Voldman applied BSA-treated hydrophobic PDMS to effectively relieve the adherent of cells [33]. Some other strategies with respect to effectively diminish the sedimentation of cells have been reported, such as coating channels with poly(dimethylacryl amide) (PDMA) [34], functionalizing the glass surface with poly(ethylene glycol) (PEG) [35] or adding HPMC to the cell suspension to increase the density of the medium [21]. In our experiments, 0.4% HPMC was added to the cell suspension to minimize the effects of wall adsorption, cell adhesion and sedimentation.

Fig. 4 shows the capture efficiency of CD4⁺ T lymphocytes within five reaction chambers. The capture efficiency was promoted from less than 10–91%, because the interaction time between target cells and antibody-coated magnetic beads was increased by using the enlarged reaction chamber. Consequently, the cell capture on dis-

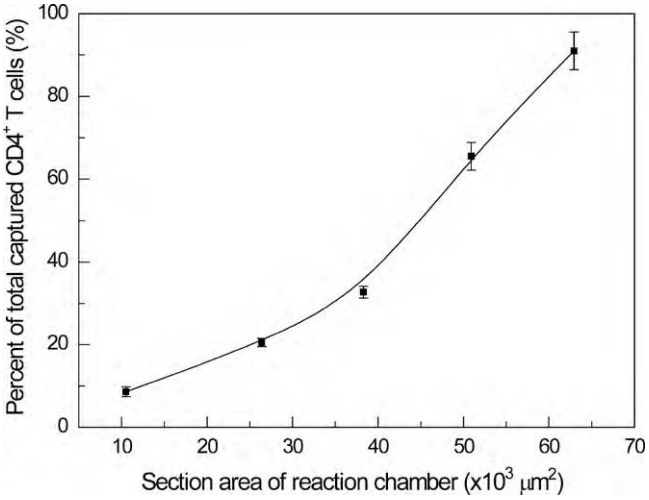

Fig. 4. Dependence of the CD4⁺ T lymphocyte capture efficiency on the five microfluidic devices. The flow rate of cell injection was 0.1 μL min^{-1}. These experiments were performed using 1 μL lymphocyte suspension from spleen or thymus of mouse. The standard error bars mean the variation of three individual experiments in a same device.

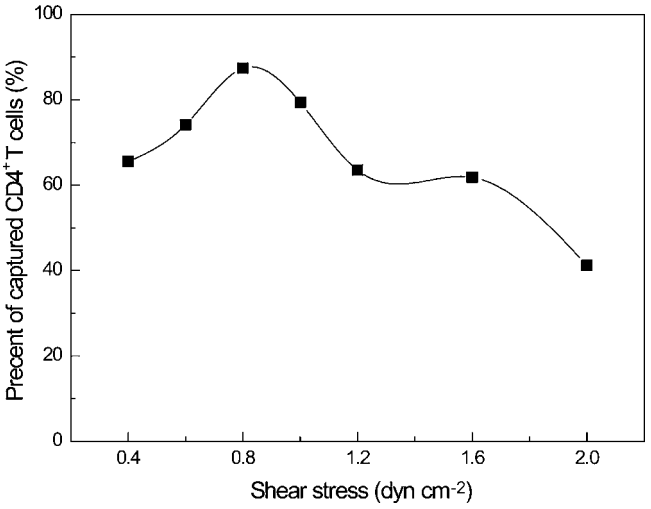

Fig. 5. Dependence of the CD4⁺ T lymphocyte capture efficiency on shear stress in a microfluidic device with the largest reaction chamber.

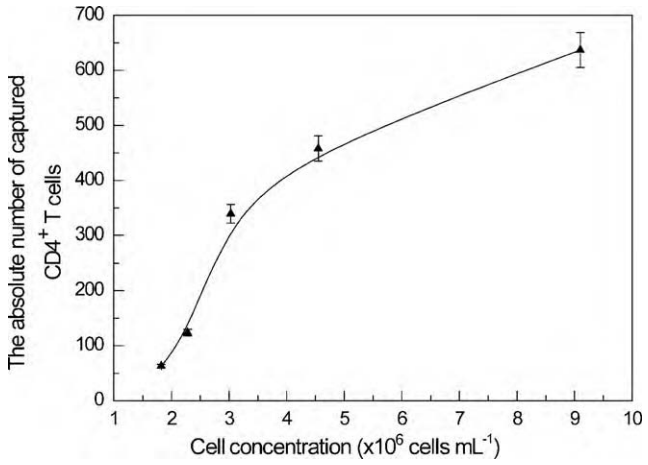

Fig. 6. Cell concentration dependency of the absolute number of captured CD4⁺ T lymphocytes. The standard error bars mean the variation of three individual experiments in a same device.

persed magnetic beads in an enlarged reaction chamber appeared to be an attractive alternative. Although CD4 molecules are present on both lymphocytes and monocytes, CD4 antigen densities are lower on monocytes [36]. We could differentiate them by controlling the shear stress acting on the cells. Therefore, we did not need to use another method to identify monocytes in this work.

3.3. *Effect of flow rate on CD4⁺ T lymphocyte capture efficiency*

In the above experiments, we demonstrated selective capture of CD4⁺ T lymphocytes from lymphocyte suspension using magnetic beads within reaction chambers under different shear stress, and illustrated that the largest reaction chamber was the most appropriate design. Next, we used the largest reaction chamber to test the effect of flow rate (0.1–0.5 $\mu L\,min^{-1}$) on the cell capture efficiency. The concentration of the cells introduced into the channel was about 3.4×10^6 cells mL^{-1}. Lower flow rate leads to longer reaction time, so more CD4⁺ T lymphocytes could be captured. Fig. 5 shows the relationship between shear stress and capture efficiency. The results indicated that a shear stress of 0.8 dyn cm^{-2} in the largest reaction chamber was optimal for CD4⁺ T lymphocytes capture. In addition, the capture efficiency decreased with the shear stress increasing from 1.0 dyn cm^{-2} to 1.6 dyn cm^{-2}. When the shear stress increased up to 2.0 dyn cm^{-2}, the capture efficiency decreased to as low as 41%. In order to confirm the method could work well under best conditions or not, we further performed a dilution control study to evaluate the correlation between cell concentration and the absolute number of captured CD4⁺ T lymphocytes at the constant flow rate of 0.2 $\mu L\,min^{-1}$, which corresponds to a shear stress of ~0.8 dyn cm^{-2}. Different concentrations of cell suspensions were tested to compare the capture efficiencies of off-line and on-line. The results are shown in Table 1. The standard deviation of less than 4% indicated the high reproducibility for different runs on the same chip and between different chips.

Table 1
CD4⁺ T lymphocyte capture efficiency compared with off-line and on-line.

Cell concentration	CD4⁺ T lymphocyte capture efficiency	
	Off-line (%)	On-line (%)
2.0×10^6	93.7 ± 2.2	90.1 ± 1.8
3.4×10^6	91.4 ± 3.1	87.4 ± 4.0
4.8×10^6	92.6 ± 1.8	88.5 ± 3.2
7.2×10^6	90.6 ± 3.4	87.3 ± 2.5

And a microfluidic device could be used at least 10 times without reducing the capture efficiency. Another stock concentration of cell suspension of 9.1×10^6 cells mL^{-1} was used to determine the absolute number of captured CD4⁺ T lymphocytes. Fig. 6 shows that when the cell concentration was smaller than 3×10^6 cells mL^{-1}, the absolute CD4 count is below 200 cells μL^{-1}, which is used clinically to discriminate relevant CD4 count thresholds of AIDS. With the increasing concentration of cells, the number of captured CD4⁺ T lymphocytes increased, the maximum number of captured CD4⁺ T lymphocytes was 653 ± 32 cells μL^{-1} (the capture efficiency is 87.3 ± 4.5%). Each experiment was repeated three times in the same device under the same condition with the standard deviation of less than 4.5%.

4. Conclusions

We developed a simple, rapid and inexpensive CD4⁺ T lymphocytes isolation device based on magnetic bead bed immunoassay. The magnetic bead bed method provided a strategy to increase the capture surface area, and place cells and surface marker antibodies in closer proximity. The use of a magnetically captured bed also allowed the cells to be readily released again after washing for further sample processing. The enlarger reaction chambers not only reduced sample process time, but also diminished shear stresses in favour of retaining captured cells. Furthermore, we can design more reaction chambers in the microchip to separate specific cells simultaneously. Although the isolation of CD4⁺ T lymphocytes from mouse was taken as a model, it can also be applied to separate and enumerate human CD4⁺ T lymphocytes with the anti-human CD4 magnetic beads to monitor HIV in resource-limited settings.

Acknowledgements

This work was supported by National Natural Science Foundation of China (no. 90813015) and National Basic Research Program of China (973 Program, no. 2007CB714507).

References

[1] H.C. Lane, H. Masur, E.P. Gelmann, D.L. Longo, R.G. Steis, T. Chused, G. Whalen, L.C. Edgar, A.S. Fauci, Am. J. Med. 78 (1985) 417–422.
[2] T. Hulgan, B.E. Shepherd, S.P. Raffanti, J.S. Fusco, R. Beckerman, G. Barkanic, T.R. Sterling, J. Infect. Dis. 195 (2007) 425–431.
[3] A. Landay, B. Ohlssonwilhelm, J.V. Giorgi, AIDS 4 (1990) 479–497.
[4] D. Carriere, C. Fontaine, A.M. Berthier, A.M. Rouquette, P. Carayon, M. Laprode, R. Juillard, A. Jansen, P. Paoli, F. Paolucci, et al., Clin. Chem. 40 (1994) 30–37.

[5] D. Carriere, J.P. Vendrell, C. Fontaine, A. Jansen, J. Reynes, I. Pages, C. Holzmann, M. Laprade, B. Pau, Clin. Chem. 45 (1999) 92–97.
[6] S. Diagbouga, G. Durand, P.T. Sanou, H. Dahourou, E. Ledru, Trop. Med. Int. Health 4 (1999) 79–84.
[7] E.F. Lyamuya, C. Kagoma, E.C. Mbena, W.K. Urassa, K. Pallangyo, F.S. Mhalu, G. Biberfeld, J. Immunol. Methods 195 (1996) 103–112.
[8] L.P. Sun, M. Zborowski, L.R. Moore, J.J. Chalmers, Cytometry 33 (1998) 469–475.
[9] E. Tamaki, K. Sato, M. Tokeshi, K. Sato, M. Aihara, T. Kitamori, Anal. Chem. 74 (2002) 1560–1564.
[10] M.S. Yang, C.W. Li, J. Yang, Anal. Chem. 74 (2002) 3991–4001.
[11] W.H. Huang, W. Cheng, Z. Zhang, D.W. Pang, Z.L. Wang, J.K. Cheng, D.F. Cui, Anal. Chem. 76 (2004) 483–488.
[12] J. Gao, X.F. Yin, Z.L. Fang, Lab Chip 4 (2004) 47–52.
[13] V.I. Furdui, D.J. Harrison, Lab Chip 4 (2004) 614–618.
[14] D.W. Inglis, R. Riehn, R.H. Austin, J.C. Sturm, Appl. Phys. Lett. 85 (2004) 5093–5095.
[15] D.C. Pregibon, M. Toner, P.S. Doyle, Langmuir 22 (2006) 5122–5128.
[16] N.N. Mishra, S. Retterer, T.J. Zieziulewicz, M. Isaacson, D. Szarowski, D.E. Mousseau, D.A. Lawrence, J.N. Turner, Biosens. Bioelectron. 21 (2005) 696–704.
[17] X. Cheng, Y.S. Liu, D. Irimia, U. Demirci, L.J. Yang, L. Zamir, W.R. Rodriguez, M. Toner, R. Bashir, Lab Chip 7 (2007) 746–755.
[18] D.K. Wood, G.B. Braun, J.L. Fraikin, L.J. Swenson, N.O. Reich, A.N. Cleland, Lab Chip 7 (2007) 469–474.
[19] Y.N. Wang, Y.J. Kang, D.Y. Xu, C.H. Chon, L. Barnett, S.A. Kalams, D.Y. Li, D.Q. Li, Lab Chip 8 (2008) 309–315.
[20] A. Ozcan, U. Demirci, Lab Chip 8 (2008) 98–106.
[21] B. Yao, G.A. Luo, X. Feng, W. Wang, L.X. Chen, Y.M. Wang, Lab Chip 4 (2004) 603–607.
[22] D.W. Inglis, J.A. Davis, T.J. Zieziulewicz, D.A. Lawrence, R.H. Austin, J.C. Sturm, J. Immunol. Methods 329 (2008) 151–156.
[23] S. Thorslund, R. Larsson, F. Nikolajeff, J. Bergquist, J. Sanchez, Sens. Actuators B: Chem. 123 (2007) 847–855.
[24] W.R. Rodriguez, N. Christodoulides, P.N. Floriano, S. Graham, S. Mohanty, M. Dixon, M. Hsiang, T. Peter, S. Zavahir, I. Thior, D. Romanovicz, B. Bernard, A.P. Goodey, B.D. Walker, J.T. McDevitt, PLoS Med. 2 (2005) 663–672.
[25] X.H. Cheng, D. Irimia, M. Dixon, K. Sekine, U. Demirci, L. Zamir, R.G. Tompkins, W. Rodriguez, M. Toner, Lab Chip 7 (2007) 170–178.
[26] A. Sin, S.K. Murthy, A. Revzin, R.G. Tompkins, M. Toner, Biotechnol. Bioeng. 91 (2005) 816–826.
[27] H.S. Kim, O.T. Son, K.H. Kim, S.H. Kim, S. Maeng, H.I. Jung, Biotechnol. Lett. 29 (2007) 1659–1663.
[28] N. Xia, T.P. Hunt, B.T. Mayers, E. Alsberg, G.M. Whitesides, R.M. Westervelt, D.E. Ingber, Biomed. Microdevices 8 (2006) 299–308.
[29] M. Herrmann, T. Veres, M. Tabrizian, Lab Chip 6 (2006) 555–560.
[30] J.J. Liu, D. Gao, H.F. Li, J.M. Lin, Lab Chip 9 (2009) 1301–1305.
[31] Y. Francois, K. Zhang, A. Varenne, P. Gareil, Anal. Chim. Acta 562 (2006) 164–170.
[32] K. Liu, R. Pitchimani, D. Dang, K. Bayer, T. Harrington, D. Pappas, Langmuir 24 (2008) 5955–5960.
[33] J.R. Kovac, J. Voldman, Anal. Chem. 79 (2007) 9321–9330.
[34] M.A. McClain, C.T. Culbertson, S.C. Jacobson, J.M. Ramsey, Anal. Chem. 73 (2001) 5334–5338.
[35] G.M. Harbers, K. Emoto, C. Greef, S.W. Metzger, H.N. Woodward, J.J. Mascali, D.W. Grainger, M.J. Lochhead, Chem. Mater. 19 (2007) 4405–4414.
[36] K. Wang, B. Cometti, D. Pappas, Anal. Chim. Acta 601 (2007) 1–9.